

Electromagnetic form factors of the nucleon in the chiral quark soliton model

Chr.V. Christov^{*a,†}, A.Z. Górska^{b,‡}, K. Goeke^{a,§} and P.V. Pobylitsa^{c,***}

^a*Institut für Theoretische Physik II, Ruhr-Universität Bochum, D-44780 Bochum, Germany*

^b*Institute of Nuclear Physics, Radzikowskiego 152, 31-342 Cracow, Poland*

^c*Petersburg Nuclear Physics Institute, Gatchina, St.Petersburg 188350, Russia*

In this paper we present the derivation as well as the numerical results for the electromagnetic form factors of the nucleon within the chiral quark soliton model in the semiclassical quantization scheme. The model is based on semibosonized SU(2) Nambu – Jona-Lasinio lagrangean, where the boson fields are treated as classical ones. Other observables, namely the nucleon mean squared radii, the magnetic moments, and the nucleon- Δ splitting are calculated as well. The calculations have been done taking into account the quark sea polarization effects. The final results, including rotational $1/N_c$ corrections, are compared with the existing experimental data, and they are found to be in a good agreement for the constituent quark mass of about 420 MeV. The only exception is the neutron electric form factor which is overestimated.

PACS number(s):12.39.Fe,13.40.Em,13.40.Gp,14.20.Dh

^{*}Permanent address: Institute for Nuclear Research and Nuclear Energy, Sofia, Bulgaria

[†]christov@neutron.tp2.ruhr-uni-bochum.de

[‡]gorski@bron.ifj.edu.pl

[§]goeke@hadron.tp2.ruhr-uni-bochum.de

^{***}maxpol@lnpi.spb.su

I. INTRODUCTION

In the last years one of the most challenging problems in elementary particle physics seems to be the solution of QCD in the low energy region. The main difficulties are due to the non-perturbative effects caused by the growing effective coupling constant of the fundamental theory in the low energy limit. This prevents one from using the well-known main tool of theoretical physics — the perturbation theory. Because of this, the most intriguing features of QCD, confinement and chiral symmetry breaking, still remain conceptual and practical problems.

The above mentioned obstacles have initiated an increasing interest in non-perturbative methods and effective low-energy models of hadrons. The effective models are expected to mimic the behavior of QCD at low energies.

The simplest purely fermionic Lorentz invariant model describing spontaneous chiral symmetry breakdown is the Nambu–Jona-Lasinio (NJL) model [1]. The NJL lagrangean contains chirally invariant local four-fermion interaction. In its simplest $SU(2)$ form it has the following structure:

$$\mathcal{L}_{NJL} = \bar{\Psi} (i\partial - m_0) \Psi + \frac{G}{2} [(\bar{\Psi} \Psi)^2 + (\bar{\Psi} i\vec{\tau} \gamma_5 \Psi)^2] , \quad (1)$$

where Ψ is the quark field, G is the coupling constant, $\vec{\tau}$ are the Pauli matrices in the isospin space and m_0 is the current mass the same for both *up* and *down* quarks.

Applying the well known bosonization procedure [2] the NJL model is expressed in terms of auxiliary meson fields $\sigma, \vec{\pi}$:

$$\bar{\Psi} [i\partial - m_0 - g(\sigma + i\vec{\pi} \cdot \vec{\tau} \gamma_5)] \Psi - \frac{g^2}{2G} (\sigma^2 + \vec{\pi}^2) . \quad (2)$$

Here, g is the physical pion–quark coupling constant implying that $\vec{\pi}$ are the physical pion fields. We assume that the meson fields are constrained to the chiral circle:

$$\sigma^2(\vec{x}) + \vec{\pi}^2(\vec{x}) = f_\pi^2 , \quad (3)$$

where $f_\pi = 93$ MeV is the pion decay constant.

In fact, an equivalent effective chiral quark meson theory [3] can be derived from the instanton model of the QCD vacuum.

In the chiral quark soliton model [4,5,6] based on the lagrangean (2) (frequently referred to simply as NJL model) the baryons appear as a bound state of N_c valence quarks, coupled to the polarized Dirac sea. Actually, the baryon solution of the model is obtained in two steps. In the first step, motivated by the large N_c limit, a static localized solution (soliton) is found by solving the corresponding equations of motion in an iterative self-consistent procedure [5,6], assuming that the σ and $\vec{\pi}$ fields have hedgehog structure. However, this hedgehog soliton does not preserve the spin and isospin. In order to describe the nucleon properties one needs nucleon states with proper spin and isospin numbers. To this end, making use of the rotational zero modes, the soliton is quantized [4,7]. Within the semiclassical quantization scheme quite successful calculations have been reported for the nucleon-delta mass splitting [8] and axial-vector form factor [9] as well as some results for the nucleon electric form factors [10]. Very recently, in the semiclassical quantization procedure important $1/N_c$ rotational corrections have been derived [11] for isovector magnetic moment as well as for the axial coupling constant. These corrections are derived in a formalism [11], based on the path integral approach [4]. The scheme involves a time-ordering of collective operators which follows from the collective path integral. It improves considerably the theoretical values for the isovector magnetic moment, which is strongly underestimated [12] in the leading order.

Besides its numerical success, there are also theoretical reasons why the NJL model, described by lagrangean (2), is considered as the one of the most promising effective theories describing low energy QCD phenomena.

First, the model is the simplest quark model describing spontaneous breaking of the chiral symmetry, a basic feature of QCD. This allows to treat the pions as Goldstone particles and to include familiar methods of the current algebra into the model. As for the confinement, which is absent in the model, some recent lattice QCD results for the vacuum correlation functions of hadronic currents [13] suggest that the confinement mechanism seems to have little impact on the light hadron structure, in particular on the nucleon and Delta structure.

Second, there are various hints [3,14,15] that the NJL-type lagrangean can be obtained from QCD in various low-energy approximations. It should be stressed that the large N_c limit plays a prominent role in those considerations.

The aim of this paper is to calculate the electromagnetic nucleon form factors within the $SU(2)$ chiral quark soliton model, based on the semibosonized NJL-type lagrangean, where the vacuum polarization effects taken into account. The calculations done in the semiclassical quantization scheme will include the rotational $1/N_c$ corrections, which have been shown [11] to be important for the isovector magnetic moment. In the derivation of the matrix element

of the electromagnetic current in the semiclassical quantization scheme not-commuting collective operators appear and the final result depends on the ordering of these operators. In fact, similar to ref. [11] the problem of the proper ordering of the collective operators is solved in the present paper using a path-integral approach [4] to the semiclassical quantization, which allows a natural access to the problem. This scheme allows to calculate the nucleon electromagnetic form factors, as well as such quantities like the electric mean squared radii, the magnetic moments, the nucleon- Δ energy splitting, and the electric and magnetic charge distributions of the nucleon.

The paper is organized as follows. In Section 2 we derive general expressions for the nucleon form factors in the NJL model. They are split in Dirac sea and valence quark contributions both including rotational corrections, coming from the expansion of the effective action in powers of the angular velocity of the soliton. Since the NJL model is non-renormalizable an ultraviolet regularization, which preserves the electromagnetic gauge invariance, is introduced in Section 3. The general formalism developed in Sections 2 and 3 is then applied to evaluate the nucleon electromagnetic form factors in Section 4. In Section 5 we present and discuss our numerical results.

II. DIRAC SEA AND VALENCE QUARK CONTRIBUTIONS TO NUCLEON FORM FACTORS

Our main goal in this section is to derive a general formula for nucleon form factors in the NJL model including rotational corrections. We start with the path integral representation for the nucleon matrix element of the corresponding quark current. After integrating out the quark fields we find that the result splits in two parts, the Dirac sea and the valence quark contributions. Usually the remaining integral over the meson fields is evaluated within the saddle point approximation. However, the saddle-point classical solution has a hedgehog symmetry that breaks both rotational and $SU(2)$ isospin symmetries. In order to restore them one has to consider a rotating soliton and to perform a functional integration over the time-dependent orientation matrix of the soliton. Expanding in powers of the angular velocity up to linear order we derive rotational corrections to the nucleon form factors. A special attention is paid to the correct ordering of non-commuting collective operators describing the rotational degrees of freedom of the soliton. In this section the consideration is limited to the non-regularized case and the ultraviolet regularization is postponed till Section 3.

Under the chiral circle restriction (3) we can introduce the $SU(2)$ chiral meson field

$$U = \frac{1}{f_\pi}(\sigma + i\vec{\pi} \cdot \vec{\tau}) \quad (4)$$

and work with the Euclidean lagrangean

$$L = \Psi^\dagger D(U) \Psi, \quad (5)$$

where the operator

$$D(U) = \gamma_4(\gamma_\mu \partial_\mu + MU^{\gamma_5} + m_0) = \partial_\tau + h(U) \quad (6)$$

includes the Euclidean time derivative ∂_τ ($\tau = x_4$) and the Dirac one-particle hamiltonian reads:

$$h(U) = \gamma_4(\gamma_k \partial_k + MU^{\gamma_5} + m_0). \quad (7)$$

Here $M = gf_\pi$ is the constituent quark mass. For convenience, we choose to work with hermitean Euclidean Dirac matrices $\gamma_\alpha^\dagger = \gamma_\alpha$. We use notation

$$U^{\gamma_5} = \frac{1 + \gamma_5}{2}U + \frac{1 - \gamma_5}{2}U^\dagger. \quad (8)$$

The aim of this paper is to calculate the electromagnetic nucleon form factors. However, to be more general we start with a matrix element of quark current $\Psi^\dagger O \Psi$, where O is some matrix with spin and isospin indices, and represent this matrix element by the Euclidean functional integral [4] with the lagrangean (5):

$$\begin{aligned} \langle N', \vec{p}' | \Psi^\dagger(0) O \Psi(0) | N, \vec{p} \rangle &= \lim_{T \rightarrow +\infty} \frac{1}{Z} \int d^3x d^3y e^{-i\vec{p}' \vec{x}' + i\vec{p} \vec{x}} \\ &\int \mathcal{D}U \int \mathcal{D}\Psi \int \mathcal{D}\Psi^\dagger J_{N'}(\vec{x}', -T/2) \Psi^\dagger(0) O \Psi(0) J_N^\dagger(\vec{x}, T/2) e^{-\int d^4z \Psi^\dagger D(U) \Psi}. \end{aligned} \quad (9)$$

Here the nucleon state is created by the nucleon current $J_N^\dagger(x)$ constructed of N_c (number of colors) quark fields Ψ

$$J_N(x) = \frac{1}{N_c!} \epsilon^{c_1 \dots c_{N_c}} \Gamma_{JJ_3, TT_3}^{\{\alpha_1 \dots \alpha_{N_c}\}} \Psi_{c_1 \alpha_1}(x) \dots \Psi_{c_{N_c} \alpha_{N_c}}(x) \quad (10)$$

where c_i are color indices and $\Gamma_{JJ_3, TT_3}^{\{\alpha_1 \dots \alpha_{N_c}\}}$ is a matrix with α_i standing for both flavor and spin indices. J and T denote the nucleon spin and isospin, respectively. In the limit of large Euclidean times x'_4, x_4 only the lowest nucleon state survives in (9).

We assume that the constant Z in eq. (9) is chosen so that the nucleon states obey the non-relativistic normalization condition:

$$\langle N, \vec{p}' | N, \vec{p} \rangle = (2\pi)^3 \delta^{(3)}(\vec{p}' - \vec{p}). \quad (11)$$

Let us integrate the quarks out in (9). The result is naturally split in valence and Dirac sea parts (see Fig.1):

$$\langle N', \vec{p}' | \Psi^\dagger O \Psi | N, \vec{p} \rangle = \langle N', \vec{p}' | \Psi^\dagger O \Psi | N, \vec{p} \rangle^{sea} + \langle N', \vec{p}' | \Psi^\dagger O \Psi | N, \vec{p} \rangle^{val}, \quad (12)$$

where

$$\begin{aligned} \langle N', \vec{p}' | \Psi^\dagger O \Psi | N, \vec{p} \rangle^{sea} &= N_c \lim_{T \rightarrow +\infty} \frac{1}{Z} \int d^3x d^3y e^{-i\vec{p}' \vec{x}' + i\vec{p} \vec{x}} \\ &\times \int \mathcal{D}U \Gamma_{N'}^{\beta_1 \dots \beta_{N_c}} \Gamma_N^{\alpha_1 \dots \alpha_{N_c}*} \prod_{k=1}^{N_c} \langle x', T/2 | \frac{1}{D(U)} | x, -T/2 \rangle_{\beta_k \alpha_k} \text{Sp} \left\{ O_{\gamma \gamma'} \langle 0, 0 | \frac{-1}{D(U)} | 0, 0 \rangle_{\gamma' \gamma} \right\} \\ &\times e^{N_c \text{Tr} \log[D(U)]} \end{aligned} \quad (13)$$

and

$$\begin{aligned} \langle N', \vec{p}' | \Psi^\dagger O \Psi(0) | N, \vec{p} \rangle^{val} &= N_c \lim_{T \rightarrow +\infty} \frac{1}{Z} \int d^3x d^3y e^{-i\vec{p}' \vec{x}' + i\vec{p} \vec{x}} \\ &\times \int \mathcal{D}U \Gamma_{N'}^{\beta_1 \dots \beta_{N_c}} \Gamma_N^{\alpha_1 \dots \alpha_{N_c}*} \prod_{k=2}^{N_c} \langle \vec{x}', T/2 | \frac{1}{D(U)} | \vec{x}, -T/2 \rangle_{\beta_k \alpha_k} \\ &\times \langle x', T/2 | \frac{1}{D(U)} | 0, 0 \rangle_{\beta_1 \gamma} O_{\gamma \gamma'} \langle 0, 0 | \frac{1}{D(U)} | \vec{x}, -T/2 \rangle_{\gamma' \alpha_1} e^{N_c \text{Tr} \log[D(U)]}. \end{aligned} \quad (14)$$

In the limit of large number of colors N_c the functional integrals over the chiral field $U(x)$ in eqs. (13), (14) can be evaluated by the saddle point method. The saddle point solution \bar{U} is a static localized field configuration with the hedgehog symmetry

$$\bar{U}(x) = e^{iP(|\vec{x}|)(x^a \tau^a)/|\vec{x}|}, \quad (15)$$

where $P(|\vec{x}|)$ is the profile function of the soliton. This saddle point solution breaks the space rotational and isospin symmetries. Therefore, even in the leading order in N_c , one should go beyond the field \bar{U} , extending the path integral over all fields of the form:

$$U(x) = R(x_4) \bar{U}(\vec{x}) R^\dagger(x_4), \quad (16)$$

where $R(x_4)$ is the time-dependent $SU(2)$ orientation matrix of the soliton.

For this ansatz (16) the operator $D(U)$ (6) can be written as

$$D(U) = R [D(\bar{U}) + R^\dagger \dot{R}] R^\dagger. \quad (17)$$

The dot stands for the derivative with respect to the Euclidean time x_4 . Similarly, the quark propagator in the background meson field U can be rewritten as

$$\langle x | \frac{1}{D(U)} | x' \rangle = R(x_4) \langle x | \frac{1}{D(\bar{U}) + R^\dagger \dot{R}} | x' \rangle R^\dagger(x_4). \quad (18)$$

Let us insert ansatz (16) into our formulas for the matrix element (13), (14) and replace the functional integral over $U(x)$ by the integral over the time dependent orientation matrix $R(x_4)$:

$$\begin{aligned}
\langle N', \vec{p}' | \Psi^\dagger O \Psi | N, \vec{p} \rangle^{sea} &= N_c \lim_{T \rightarrow +\infty} \frac{1}{Z} \int d^3x d^3y e^{-i\vec{p}'\vec{x}' + i\vec{p}\vec{x}} \\
&\times \int \mathcal{D}R \Gamma_{N'}^{\beta_1 \dots \beta_{N_c}} \Gamma_N^{\alpha_1 \dots \alpha_{N_c}*} \prod_{k=1}^{N_c} \left[R(T/2) \langle \vec{x}', T/2 | \frac{1}{D(U)} | \vec{x}, -T/2 \rangle R^\dagger(-T/2) \right]_{\beta_k \alpha_k} \\
&\times \text{Sp} \left\{ O_{\gamma\gamma'} \left[R(0) \langle 0, 0 | \frac{-1}{D(U)} | 0, 0 \rangle R^\dagger(0) \right]_{\gamma'\gamma} \right\} e^{N_c \text{Tr} \log[D(\bar{U}) + R^\dagger \dot{R}]} \tag{19}
\end{aligned}$$

and

$$\begin{aligned}
\langle N', \vec{p}' | \Psi^\dagger O \Psi(0) | N, \vec{p} \rangle^{val} &= N_c \lim_{T \rightarrow +\infty} \frac{1}{Z} \int d^3x d^3y e^{-i\vec{p}'\vec{x}' + i\vec{p}\vec{x}} \\
&\times \int \mathcal{D}R e^{N_c \text{Tr} \log[D(\bar{U}) + R^\dagger \dot{R}]} \Gamma_{N'}^{\beta_1 \dots \beta_{N_c}} \Gamma_N^{\alpha_1 \dots \alpha_{N_c}*} \prod_{k=2}^{N_c} \left[R(T/2) \langle \vec{x}', T/2 | \frac{1}{D(U)} | \vec{x}, -T/2 \rangle R^\dagger(-T/2) \right]_{\beta_k \alpha_k} \\
&\times \left[R(T/2) \langle \vec{x}', T/2 | \frac{1}{D(U)} | 0, 0 \rangle R^\dagger(0) \right]_{\beta_1 \gamma} O_{\gamma\gamma'} \left[\langle 0, 0 | \frac{1}{D(U)} | \vec{x}, -T/2 \rangle R^\dagger(-T/2) \right]_{\gamma' \alpha_1}. \tag{20}
\end{aligned}$$

In eqs. (19), (20) despite of ansatz (16) we still have a complicated path integral over $\mathcal{D}R$. In order to solve this problem we make essentially use that in the large N_c limit the angular velocity $R^\dagger \dot{R}$ of the soliton as well as its derivative is suppressed [4]. Hence, similarly to ref. [4] we can use expansions in powers of it

$$N_c \text{Tr} \log[D(\bar{U}) + R^\dagger \dot{R}] = N_c \text{Tr} \log[D(\bar{U})] + \Theta^{sea} \int d\tau \text{Sp}(R^\dagger \dot{R})^2 + \dots, \tag{21}$$

and

$$\frac{1}{D(\bar{U}) + R^\dagger \dot{R}} = \frac{1}{D(\bar{U})} - \frac{1}{D(\bar{U})} R^\dagger \dot{R} \frac{1}{D(\bar{U})} + \dots. \tag{22}$$

In eq.(21) the second term of the action is a function of the angular velocity only. As we will see later, the coefficient Θ^{sea} is the Dirac sea contribution to the moment of inertia of the soliton.

Using the expansions (21),(22), in eqs. (19), (20) up to terms quadratic in $R^\dagger \dot{R}$ we arrive at a functional integral over the time dependent orientation matrices $R(x_4)$ with the action quadratic in angular velocities [4]. In large N_c limit, the latter corresponds to the hamiltonian of the quantum spherical rotator:

$$H_{rot} = J_a^2 / (2\Theta), \tag{23}$$

It means that despite of the fact that in general the path integral over R runs over all possible trajectories, in large N_c limit the main contribution comes from trajectories close to those of the quantum rotator with hamiltonian (23). In eq. (23) J_a is the spin operator of the nucleon and

$$\Theta = \Theta^{sea} + \Theta^{val} \tag{24}$$

is the total moment of inertia, including also the valence quark contribution Θ^{val} — see eq. (80) below. According to eq. (23) the quantization rule (for the Euclidean time) is given by

$$\text{Sp}(R^\dagger \dot{R} \tau_a) \rightarrow \frac{J_a}{\Theta}, \tag{25}$$

We also make use of the identity

$$R^\dagger \dot{R} = \frac{1}{2} \text{Sp}(R^\dagger \dot{R} \tau_a) \tau^a \tag{26}$$

in order to separate the part, acting on the rotational functions of the nucleon $\psi_N(R)$, from the Pauli matrices τ^a which act in the isospin space of the quark states.

It should be also noted that in expansions (21) and (22) we have neglected the terms containing derivatives of angular velocity $\partial_\tau(R^\dagger \dot{R})$. Such a treatment is consistent in a sense that for the hamiltonian (23) we have

$$\partial_\tau(R^\dagger \dot{R}) = [H_{rot}, R^\dagger \dot{R}] = 0 \tag{27}$$

for any rotation state of H_{rot} .

After quantization (25) we have to deal with not-commuting collective operators. Apparently, since the path integral corresponds to the following operator construction:

$$\int_{R(T_1)=R_1}^{R(T_2)=R_2} \mathcal{D}R F_1(R(t_1)) \cdots F_n(R(t_n)) e^{-S(R)} = \langle R_2, T_2 | \mathcal{T}\{\hat{F}_1(R(t_1)) \cdots \hat{F}_n(R(t_n))\} | R_1, T_1 \rangle, \quad (28)$$

where \mathcal{T} stands for time-ordering of operators $\hat{F}_n(R(t_n))$ in the Heisenberg representation, the order of the collective operators, which appear after the integration over R , is strictly fixed by the time ordering.

Back to the sea contribution (19), expanding both the action and the integrand in powers of $R^\dagger \dot{R}$ and performing the functional integration over time dependent $R(x_4)$ in large N_c limit, we now have

$$\langle N', \vec{p}' | \Psi^\dagger O \Psi | N, \vec{p} \rangle^{sea} = N_c \int d^3x e^{i(\vec{p}' - \vec{p}) \vec{x}} \int dR \psi_{N'}^*(R) \text{Sp} \left[R^\dagger O R \langle \vec{x}, 0 | \frac{-1}{D(\bar{U}) + R^\dagger \dot{R}} | \vec{x}, 0 \rangle \right] \Big|_{\text{Sp}(R^\dagger \dot{R} \tau_a) \xrightarrow{\mathcal{T}} J_a / \Theta} \psi_N(R), \quad (29)$$

where $\xrightarrow{\mathcal{T}}$ means again time-ordering of the collective operators. The rotational wave functions $\psi_N(R)$ comes from the product of N_c matrices $R(T/2)$, which appear in eq. (13) after transformation (18), contracted by the matrices Γ_N from the definition of the baryon current (10). For given spin J, J_3 and isospin T, T_3 these wave functions can be expressed through the Wigner D functions

$$\psi_{TT_3JJ_3}(R) = (-1)^{T+T_3} \sqrt{2T+1} D_{-T_3, J_3}^{T=J}(R). \quad (30)$$

In eq.(29) the integral over \vec{x} has appeared due to the integration over the translational modes of the soliton and the matrix element in the integrand is given by

$$\begin{aligned} \text{Sp} \left[R^\dagger O R \langle \vec{x}, 0 | \frac{-1}{D(\bar{U}) + R^\dagger \dot{R}} | \vec{x}, 0 \rangle \right] \Big|_{\text{Sp}(R^\dagger \dot{R} \tau_a) \xrightarrow{\mathcal{T}} J_a / \Theta} &= - \text{Sp} \left[R^\dagger O R \langle \vec{x}, 0 | \frac{1}{D(\bar{U})} | \vec{x}, 0 \rangle \right] \\ &+ \frac{1}{2\Theta} \text{Sp} \int d^4y [\theta(y_4) J_a R^\dagger O R + \theta(-y_4) R^\dagger O R J_a] \langle \vec{x}, 0 | \frac{1}{D(\bar{U})} | y \rangle \tau^a \langle y | \frac{1}{D(\bar{U})} | \vec{x}, 0 \rangle. \end{aligned} \quad (31)$$

As a next step we use the spectral representation for the quark propagator

$$\langle x' | \frac{1}{D(\bar{U})} | x \rangle = \theta(x'_4 - x_4) \sum_{\varepsilon_n > 0} e^{-\varepsilon_n(x'_4 - x_4)} \Phi_n(\vec{x}') \Phi_n^\dagger(\vec{x}) - \theta(x_4 - x'_4) \sum_{\varepsilon_n < 0} e^{-\varepsilon_n(x'_4 - x_4)} \Phi_n(\vec{x}') \Phi_n^\dagger(\vec{x}) \quad (32)$$

written in terms of eigenvalues ε_n and eigenfunctions Φ_n of the Dirac hamiltonian (7)

$$h(\bar{U}) \Phi_n = \varepsilon_n \Phi_n. \quad (33)$$

in order to evaluate the matrix elements and the integral over y_4 in (31). Finally we get for the sea contribution (13) the following result:

$$\begin{aligned} \langle N', \vec{p}' | \Psi^\dagger O \Psi | N, \vec{p} \rangle^{sea} &= N_c \int d^3x e^{i(\vec{p}' - \vec{p}) \vec{x}} \int dR \psi_{N'}^*(R) \left\{ \sum_{\varepsilon_n < 0} \Phi_n^\dagger(\vec{x}) R^\dagger O R \Phi_n(\vec{x}) + \frac{1}{2\Theta} \sum_{m,n} \frac{1}{\varepsilon_n - \varepsilon_m} \right. \\ &\times \left. \left\{ -\theta(\varepsilon_n) \theta(-\varepsilon_m) J_a [\Phi_n^\dagger(\vec{x}) R^\dagger O R \Phi_m(\vec{x})] + \theta(-\varepsilon_n) \theta(\varepsilon_m) [\Phi_n^\dagger(\vec{x}) R^\dagger O R \Phi_m(\vec{x})] J_a \right\} \times \langle m | \tau^a | n \rangle \right\} \psi_N(R) \end{aligned} \quad (34)$$

Now the valence level contribution to the form factor (14) is in order. Note that in the limit of large Euclidean time $T \rightarrow +\infty$ the quark propagator (32) is dominated by the contribution of the lowest level with $\varepsilon_n > 0$, i.e. by the valence quark level with the wave function $\Phi_{val}(\vec{x})$. We perform analogous calculations as in the case of Dirac sea, i.e. using the rotating ansatz (16) in (14) and expanding up to the linear order in the angular velocity with time-ordering of collective operators we arrive at the following result for the valence quark contribution:

$$\begin{aligned}
\langle N', \vec{p}' | \Psi^\dagger O \Psi | N, \vec{p} \rangle^{val} &= N_c \int d^3 x e^{i(\vec{p}' - \vec{p}) \vec{x}} \int dR \psi_{N'}^*(R) \left\{ \Phi_{val}^\dagger(\vec{x}) R^\dagger O R \Phi_{val}(\vec{x}) \right. \\
&+ \frac{1}{2\Theta} \sum_{\varepsilon_n \neq \varepsilon_{val}} \frac{1}{\varepsilon_{val} - \varepsilon_n} \left\{ \theta(\varepsilon_n) \left[J_a [\Phi_n^\dagger(\vec{x}) R^\dagger O R \Phi_{val}(\vec{x})] \langle val | \tau^a | n \rangle + [\Phi_{val}^\dagger(\vec{x}) R^\dagger O R \Phi_n(\vec{x})] \langle n | \tau^a | val \rangle J_a \right] \right. \\
&\left. \left. + \theta(-\varepsilon_n) \left[J_a [\Phi_{val}^\dagger(\vec{x}) R^\dagger O R \Phi_n(\vec{x})] \langle n | \tau^a | val \rangle + [\Phi_n^\dagger(\vec{x}) R^\dagger O R \Phi_{val}(\vec{x})] \langle val | \tau^a | n \rangle J_a \right] \right\} \right\} \psi_N(R) \quad (35)
\end{aligned}$$

Finally we add the valence contribution (35) to the sea part (34):

$$\begin{aligned}
\langle N', \vec{p}' | \Psi^\dagger O \Psi | N, \vec{p} \rangle &= N_c \int d^3 x e^{i(\vec{p}' - \vec{p}) \vec{x}} \int dR \psi_{N'}^*(R) \left\{ \sum_{\varepsilon_n \leq \varepsilon_{val}} \Phi_n^\dagger(\vec{x}) R^\dagger O R \Phi_n(\vec{x}) \right. \\
&- \frac{1}{2\Theta} \sum_{\substack{\varepsilon_n > \varepsilon_{val} \\ \varepsilon_m \leq \varepsilon_{val}}} \frac{1}{\varepsilon_n - \varepsilon_m} \left\{ J_a [\Phi_n^\dagger(\vec{x}) R^\dagger O R \Phi_m(\vec{x})] \langle m | \tau^a | n \rangle + [\Phi_m^\dagger(\vec{x}) R^\dagger O R \Phi_n(\vec{x})] \langle n | \tau^a | m \rangle J_a \right\} \right\} \psi_N(R) \quad (36)
\end{aligned}$$

It is easy to see that the result has the same structure as the sea contribution but with the valence quark included into the occupied states.

III. REGULARIZATION

The NJL model is not renormalizable. Even in the leading order of the saddle point approximation one faces ultraviolet divergences. The integrand in the r.h.s. of eq. (13) contains fermionic determinant $\text{Det}[D(U)]$ and a matrix element:

$$\text{Sp } O \langle 0 | \frac{-1}{D(U)} | 0 \rangle = \frac{\delta}{\delta \epsilon(0)} \text{Tr} \log[D(U) - \epsilon O] \Big|_{\epsilon=0} \quad (37)$$

both divergent. Apparently, in order to make it finite it is sufficient to regularize

$$\text{Tr} \log D_\epsilon \equiv \text{Tr} \log[D(U) - \epsilon O] = \text{Tr} \log[D(\bar{U}) + R^\dagger \dot{R} - \epsilon R^\dagger O R]. \quad (38)$$

In fact, we are interested in a particular operator O , for which only the real part of $\text{Tr} \log D_\epsilon$ is divergent. The corresponding regularized sea contribution to the matrix element (13) has the form

$$\langle N', \vec{p}' | \Psi^\dagger O \Psi | N, \vec{p} \rangle_{reg}^{sea} = N_c \int d^3 x e^{i(\vec{p}' - \vec{p}) \vec{x}} \int dR \psi_{N'}^*(R) \left[\frac{\delta}{\delta \epsilon(\vec{x}, 0)} \text{Re}(\text{Tr} \log D_\epsilon)_{reg} \right] \Big|_{\text{Sp}(R^\dagger \dot{R} \tau_a) \vec{J}_a / \Theta} \psi_N(R), \quad (39)$$

where we used a proper-time regularization

$$\begin{aligned}
\text{Re}(\text{Tr} \log D_\epsilon)_{reg} &\equiv \frac{1}{2} [\text{Tr} \log(D_\epsilon^\dagger D_\epsilon)]_{reg} \\
&= -\frac{1}{2} \int_{1/\Lambda^2}^{\infty} \frac{du}{u} \text{Tr} \left[e^{-uD_\epsilon^\dagger D_\epsilon} - e^{-uD_0^\dagger D_0} \right]. \quad (40)
\end{aligned}$$

Hence

$$\begin{aligned}
\frac{\delta}{\delta \epsilon(x)} \text{Re}(\text{Tr} \log D_\epsilon)_{reg} &= -\frac{1}{2} \text{Sp } R^\dagger(x_4) O R(x_4) \langle x | e^{-D^\dagger D / \Lambda^2} D^{-1} | x \rangle \\
&- \frac{1}{2} \text{Sp } R^\dagger(x_4) O^\dagger R(x_4) \langle x | (D^\dagger)^{-1} e^{-D^\dagger D / \Lambda^2} | x \rangle. \quad (41)
\end{aligned}$$

Here D stands for

$$D = D_{\epsilon=0} = \partial_\tau + h(\bar{U}) + R^\dagger \dot{R} \quad (42)$$

Note that we assume $\epsilon(x)$ to be real but the matrix O is not necessarily hermitean.

Using the expansion

$$D^{-1} = \frac{1}{\partial_\tau + h} - \frac{1}{\partial_\tau + h} R^\dagger \dot{R} \frac{1}{\partial_\tau + h} + \dots \quad (43)$$

up to the linear order in the angular velocity we get

$$\begin{aligned} e^{-D^\dagger D/\Lambda^2} &= e^{(\partial_\tau^2 - h^2)/\Lambda^2} + \frac{1}{\Lambda^2} \int_0^1 d\alpha e^{\alpha(\partial_\tau^2 - h^2)/\Lambda^2} (\partial_\tau - h) R^\dagger \dot{R} e^{(1-\alpha)(\partial_\tau^2 - h^2)/\Lambda^2} \\ &+ \frac{1}{\Lambda^2} \int_0^1 d\alpha e^{\alpha(\partial_\tau^2 - h^2)/\Lambda^2} R^\dagger \dot{R} e^{(1-\alpha)(\partial_\tau^2 - h^2)/\Lambda^2} (\partial_\tau + h) + \dots \end{aligned} \quad (44)$$

After quantization (25) of the time-ordered collective operators and using the spectral representation for the quark propagator (32) we get for the regularized Dirac sea contribution (39) in the form

$$\begin{aligned} \langle N', \vec{p}' | \Psi^\dagger O \Psi | N, \vec{p} \rangle_{reg}^{sea} &= N_c \int d^3x e^{i(\vec{p}' - \vec{p}) \cdot \vec{x}} \int dR \psi_{N'}^*(R) \left\{ \sum_n \mathcal{R}_1(\varepsilon_n, \eta) \Phi_n^\dagger(\vec{x}) R^\dagger O R \Phi_n(\vec{x}) \right. \\ &+ \left. \frac{1}{4\Theta} \sum_{m,n} \left[\mathcal{R}_2^{(+)}(\varepsilon_m, \varepsilon_n, \eta) J_a [\Phi_m^\dagger(\vec{x}) R^\dagger O R \Phi_n(\vec{x})] + \mathcal{R}_2^{(-)}(\varepsilon_m, \varepsilon_n, \eta) [\Phi_m^\dagger(\vec{x}) R^\dagger O R \Phi_n(\vec{x})] J_a \right] \langle n | \tau^a | m \rangle \right\} \psi_N(R). \end{aligned} \quad (45)$$

The coefficient $\eta = 1$ for hermitean matrix O and $\eta = -1$ for anti-hermitean one:

$$O^\dagger = \eta O. \quad (46)$$

The regularization functions are given by

$$\mathcal{R}_1(\varepsilon_n, \eta) = -\frac{1+\eta}{2} \varepsilon_n \int_{-\infty}^{\infty} \frac{d\omega}{2\pi} \frac{e[-(\omega^2 + \varepsilon_n^2)/\Lambda^2]}{\omega^2 + \varepsilon_n^2}, \quad (47)$$

$$\mathcal{R}_2^{(\pm)}(\varepsilon_m, \varepsilon_n, \eta) = \mathcal{R}^{(\pm)}(\varepsilon_m, \varepsilon_n) - \eta \mathcal{R}^{(\pm)}(\varepsilon_n, \varepsilon_m), \quad (48)$$

$$\begin{aligned} \mathcal{R}^{(\pm)}(\varepsilon_m, \varepsilon_n) &= \int_{-\infty}^{\infty} \frac{d\omega}{2\pi} \int_{-\infty}^{\infty} \frac{d\omega'}{2\pi} \frac{1}{\pm i(\omega - \omega') + 0} \frac{1}{(i\omega + \varepsilon_n)(i\omega' + \varepsilon_m)} \\ &- \frac{1}{\Lambda^2} \left[1 + \frac{i\omega - \varepsilon_n}{i\omega' + \varepsilon_m} \right] \int_0^1 d\alpha e \left[-\frac{\alpha(\omega^2 + \varepsilon_n^2) + (1-\alpha)(\omega'^2 + \varepsilon_m^2)}{\Lambda^2} \right] \} \end{aligned} \quad (49)$$

IV. ELECTROMAGNETIC FORM FACTORS

In this section we apply the formalism, developed above, to the case of the electromagnetic form factors. We pay a special attention to the ultraviolet regularization to preserve the electromagnetic gauge invariance. Following this regularization prescription we evaluate the nucleon matrix elements of the electromagnetic current in the NJL model and relate them to the Sachs form factors.

In the previous section we have presented a scheme for evaluating the regularized determinant with a small external source ϵO (37). In the case of the electromagnetic form factors this external source is an electromagnetic field A_μ :

$$D(U) - \epsilon O \rightarrow D(U, Q A_\mu) = \gamma_4 [\gamma_\mu (\partial_\mu - i Q A_\mu) + M U^{\gamma_5}]. \quad (50)$$

Here Q is the quark charge matrix

$$Q = \begin{pmatrix} 2/3 & 0 \\ 0 & -1/3 \end{pmatrix} = \frac{1}{6} + \frac{\tau^3}{2}. \quad (51)$$

Our proper-time regularization in the Euclidean space (40) includes operator $D^\dagger D$. Therefore, in order to preserve the gauge invariance in (40) the Euclidean electromagnetic field A_μ should be real.

The complex conjugate Euclidean Dirac matrices γ_μ^* are connected to γ_μ by some unitary transformation V

$$\gamma_\mu^* = V \gamma_\mu V^{-1} \quad (\mu = 1, 2, 3, 4, 5). \quad (52)$$

It is easy to show that

$$(V\tau^2)D(U, QA_\mu)(V\tau^2)^{-1} = [D(U, Q'A_\mu)]^*, \quad (53)$$

where

$$Q' = -\frac{1}{6} + \frac{\tau^3}{2} \quad (54)$$

and the asterisk stands for the complex (not hermitean!) conjugation.

Comparing Q (51) and Q' (54) we see that their isovector part remains the same whereas the isoscalar component changes the sign. The identity (53) shows that the isoscalar electromagnetic form factors originate from the imaginary part of $\text{Tr} \log D(U, QA_\mu)$ whereas the isovector form factors are generated by the real part of $\text{Tr} \log D(U, QA_\mu)$.

Since the imaginary part of $\text{Tr} \log D(U, QA_\mu)$ is ultraviolet finite, for the isoscalar form factors we use directly the non-regularized expression (36). In this case the integral over R becomes trivial and reduces to the orthogonality condition for the rotational wave functions or to the standard matrix elements of the spin operator J_a

$$\begin{aligned} \langle T'_3, J'_3, \vec{p}' | \Psi^\dagger i\gamma_4 \gamma_\mu \Psi | T_3, J_3, \vec{p} \rangle &= N_c \delta_{T'_3 T_3} \int d^3 x e^{i(\vec{p}' - \vec{p}) \vec{x}} \left\{ \delta_{J'_3 J_3} \sum_{\varepsilon_n \leq \varepsilon_{val}} \Phi_n^\dagger(\vec{x}) i\gamma_4 \gamma_\mu \Phi_n(\vec{x}) \right. \\ &\quad \left. - \frac{1}{4\Theta} (\tau^a)_{J'_3 J_3} \sum_{\substack{\varepsilon_n > \varepsilon_{val} \\ \varepsilon_m \leq \varepsilon_{val}}} \frac{1}{\varepsilon_n - \varepsilon_m} \left[[\Phi_n^\dagger(\vec{x}) i\gamma_4 \gamma_\mu \Phi_m(\vec{x})] \langle m | \tau^a | n \rangle + [\Phi_m^\dagger(\vec{x}) i\gamma_4 \gamma_\mu \Phi_n(\vec{x})] \langle n | \tau^a | m \rangle \right] \right\}. \end{aligned} \quad (55)$$

In the case of the isovector current, however, we have to use the regularized expression (45) for the sea contribution, which leads to:

$$\begin{aligned} \langle N', \vec{p}' | \Psi^\dagger i\gamma_4 \gamma_\mu \tau^3 \Psi | N, \vec{p} \rangle_{reg}^{sea} &= N_c \int d^3 x e^{i(\vec{p}' - \vec{p}) \vec{x}} \int dR \psi_{N'}^*(R) \left\{ D_{3b}(R) \sum_n \mathcal{R}_1(\varepsilon_n, \eta) \Phi_n^\dagger(\vec{x}) i\gamma_4 \gamma_\mu \tau^b \Phi_n(\vec{x}) \right. \\ &\quad \left. + \frac{1}{4\Theta} \sum_{m,n} \left[\mathcal{R}_2^{(+)}(\varepsilon_m, \varepsilon_n, \eta) J_a D_{3b}(R) + \mathcal{R}_2^{(-)}(\varepsilon_m, \varepsilon_n, \eta) D_{3b}(R) J_a \right] [\Phi_m^\dagger(\vec{x}) i\gamma_4 \gamma_\mu \tau^b \Phi_n(\vec{x})] \langle n | \tau^a | m \rangle \right\} \psi_N(R), \end{aligned} \quad (56)$$

where

$$D_{ab}(R) = \frac{1}{2} \text{Sp}(R^\dagger \tau^a R \tau^b). \quad (57)$$

Note that $i\gamma_4 \gamma_\mu \tau^b$ is hermitean for $\mu = 1, 2, 3$ and anti-hermitean for $\mu = 4$ which means that the coefficient η (defined in (46)) has the following values:

$$\eta = \begin{cases} 1 & \text{if } \mu = 1, 2, 3 \\ -1 & \text{if } \mu = 4. \end{cases} \quad (58)$$

Now the rotational matrix elements in (56) can be easily computed using

$$\langle T'_3 J'_3 | J_a | T_3 J_3 \rangle = \frac{1}{2} \delta_{T'_3 T_3} (\tau^a)_{J'_3 J_3}, \quad (59)$$

$$\langle T'_3 J'_3 | D_{ab}(R) | T_3 J_3 \rangle = -\frac{1}{3} (\tau^a)_{T'_3 T_3} (\tau^b)_{J'_3 J_3}, \quad (60)$$

From eq.(56) we find:

$$\begin{aligned} \langle T'_3, J'_3, \vec{p}' | \Psi^\dagger i\gamma_4\gamma_\mu\tau^3 \Psi | T_3, J_3, \vec{p} \rangle_{reg}^{sea} &= N_c T_3 \delta_{T'_3 T_3} \int d^3 x e^{i(\vec{p}' - \vec{p})\vec{x}} \left\{ -\frac{2}{3} (\tau^b)_{J'_3 J_3} \sum_n \mathcal{R}_1(\varepsilon_n, \eta) \Phi_n^\dagger(\vec{x}) i\gamma_4\gamma_\mu\tau^b \Phi_n(\vec{x}) \right. \\ &\quad \left. - \frac{1}{12\Theta} \sum_{m,n} \left\{ \delta_{ab} \delta_{J'_3 J_3} \left[\mathcal{R}_2^{(+)}(\varepsilon_m, \varepsilon_n, \eta) + \mathcal{R}_2^{(-)}(\varepsilon_m, \varepsilon_n, \eta) \right] + i\epsilon_{abc} (\tau^c)_{J'_3 J_3} \left[\mathcal{R}_2^{(+)}(\varepsilon_m, \varepsilon_n, \eta) - \mathcal{R}_2^{(-)}(\varepsilon_m, \varepsilon_n, \eta) \right] \right\} \right. \\ &\quad \left. \times [\Phi_m^\dagger(\vec{x}) i\gamma_4\gamma_\mu\tau^b \Phi_n(\vec{x})] \langle n | \tau^a | m \rangle \right\}. \end{aligned} \quad (61)$$

Under the transformation $V\tau^2$ (53) we have

$$(V\tau^2)\gamma_\mu(V\tau^2)^{-1} = \gamma_\mu^* = \gamma_\mu^T, \quad (V\tau^2)\tau^a(V\tau^2)^{-1} = -(\tau^a)^* = -(\tau^a)^T, \quad (62)$$

$$(V\tau^2)h(V\tau^2)^{-1} = h^* = h^T, \quad (63)$$

where the superscript T stands for the transposition in both the matrix indices and the coordinate space. The last equation shows that the eigenfunctions of h can be chosen in such a way that

$$(V\tau^2)\Phi_m(\vec{x}) = \Phi_m^*(\vec{x}) \quad (64)$$

and hence, the following relations hold:

$$\Phi_n^\dagger(\vec{x}) i\gamma_4\gamma_\mu\Phi_m(\vec{x}) \langle \text{langlem} | \tau^a | n \rangle = \eta \Phi_m^\dagger(\vec{x}) i\gamma_4\gamma_\mu\Phi_n(\vec{x}) \langle n | \tau^a | m \rangle, \quad (65)$$

$$\Phi_n^\dagger(\vec{x}) i\gamma_4\gamma_\mu\tau^a\Phi_m(\vec{x}) \langle m | \tau^a | n \rangle = -\eta \Phi_m^\dagger(\vec{x}) i\gamma_4\gamma_\mu\tau^a\Phi_n(\vec{x}) \langle n | \tau^a | m \rangle \quad (66)$$

with values for η are given in (58).

Using these symmetry properties of matrix elements we can simplify expression (55)

$$\begin{aligned} \langle T'_3, J'_3, \vec{p}' | \Psi^\dagger i\gamma_4\gamma_\mu\tau^3 \Psi | T_3, J_3, \vec{p} \rangle &= N_c \delta_{T'_3 T_3} \int d^3 x e^{i(\vec{p}' - \vec{p})\vec{x}} \left\{ \delta_{J'_3 J_3} \frac{1 - \eta}{2} \sum_{\varepsilon_n \leq \varepsilon_{val}} \Phi_n^\dagger(\vec{x}) i\gamma_4\gamma_\mu\Phi_n(\vec{x}) \right. \\ &\quad \left. - \frac{1 + \eta}{4\Theta} (\tau^a)_{J'_3 J_3} \sum_{\substack{\varepsilon_n > \varepsilon_{val} \\ \varepsilon_m \leq \varepsilon_{val}}} \frac{1}{\varepsilon_n - \varepsilon_m} \Phi_n^\dagger(\vec{x}) i\gamma_4\gamma_\mu\Phi_m(\vec{x}) \langle m | \tau^a | n \rangle \right\}. \end{aligned} \quad (67)$$

Starting from the general formula (35) analogous calculations of the non-regularized valence quark contribution to the matrix element of the isovector part of the electromagnetic current can be performed:

$$\begin{aligned} \langle T'_3, J'_3, \vec{p}' | \Psi^\dagger i\gamma_4\gamma_\mu\tau^3 \Psi | T_3, J_3, \vec{p} \rangle^{val} &= N_c T_3 \delta_{T'_3 T_3} \int d^3 x e^{i(\vec{p}' - \vec{p})\vec{x}} \left\{ -\frac{1 + \eta}{3} (\tau^b)_{J'_3 J_3} \Phi_{val}^\dagger(\vec{x}) i\gamma_4\gamma_\mu\tau^b \Phi_{val}(\vec{x}) \right. \\ &\quad \left. - \frac{1}{6\Theta} \sum_{\varepsilon_n \neq \varepsilon_{val}} \frac{1}{\varepsilon_{val} - \varepsilon_n} [\theta(\varepsilon_n) - \eta\theta(-\varepsilon_n)] [(1 - \eta)\delta_{ab} \delta_{J'_3 J_3} + (1 + \eta)i\epsilon_{abc} (\tau^c)_{J'_3 J_3}] \right. \\ &\quad \left. \times [\Phi_n^\dagger(\vec{x}) i\gamma_4\gamma_\mu\tau^b \Phi_{val}(\vec{x})] \langle val | \tau^a | n \rangle \right\}. \end{aligned} \quad (68)$$

Up to now we worked with Euclidean Dirac matrices. Since the same combination $i\gamma_4\gamma_\mu$ enters both left and right hand sides of our formulas for form factors the transition to the Minkowskian Dirac matrices is trivial — it is sufficient to replace the Euclidean $i\gamma_4\gamma_\mu$ by Minkowskian $i\gamma^0\gamma^\mu$ everywhere in eqs. (61), (67) and (68). Henceforward, we work in the Minkowski space-time.

The nucleon electromagnetic Sachs form factors are related to the matrix element of the electromagnetic current

$$j^\mu = \bar{\Psi} \gamma^\mu Q \Psi = \Psi^\dagger \gamma^0 \gamma^\mu \left(\frac{1}{6} + \frac{1}{2} \tau^3 \right) \Psi \quad (69)$$

in the standard way:

$$\langle J'_3, p' | j^0(0) | J_3, p \rangle = G_E(q^2) \delta_{J'_3 J_3}, \quad (70)$$

$$\langle J'_3, p' | j^k(0) | J_3, p \rangle = \frac{i}{2\mathcal{M}_N} \epsilon^{klm} (\tau^l)_{J'_3 J_3} q^m G_M(q^2), \quad (71)$$

where

$$q = p' - p. \quad (72)$$

The isoscalar and isovector parts of the form factors are defined by

$$G_{E(M)} = \frac{1}{2} G_{E(M)}^{T=0} + T_3 G_{E(M)}^{T=1}. \quad (73)$$

Using our result (67) for the nucleon matrix elements of the isoscalar vector current and definition (70) we find for the isoscalar electric form factor a simple result:

$$G_E^{T=0}(q^2) = \frac{N_c}{3} \int d^3x e^{i\vec{q}\vec{x}} \left\{ \sum_{\varepsilon_n \leq \varepsilon_{val}} \Phi_n^\dagger(\vec{x}) \Phi_n(\vec{x}) - \sum_{\varepsilon_n^{(0)} < 0} \Phi_n^{(0)\dagger}(\vec{x}) \Phi_n^{(0)}(\vec{x}) \right\} \quad (74)$$

Here we have to subtract the vacuum contribution which provides the correct normalization:

$$G_E^{T=0}(0) = 1 \quad (75)$$

For the electric isovector form factor from (61) and (68) we obtain:

$$G_E^{T=1}(q^2) = \frac{N_c}{6\Theta} \int d^3x e^{i(\vec{p}' - \vec{p})\vec{x}} \left\{ \sum_{m,n} \mathcal{R}_\Theta^\Lambda(\varepsilon_m, \varepsilon_n) [\Phi_m^\dagger(\vec{x}) \tau^a \Phi_n(\vec{x})] \langle n | \tau^a | m \rangle \right. \\ \left. - \sum_{\varepsilon_n \neq \varepsilon_{val}} \frac{1}{\varepsilon_{val} - \varepsilon_n} [\Phi_n^\dagger(\vec{x}) \tau^a \Phi_{val}(\vec{x})] \langle val | \tau^a | n \rangle \right\}, \quad (76)$$

where the regulator has the form:

$$\mathcal{R}_\Theta^\Lambda(\varepsilon_m, \varepsilon_n) = -\frac{1}{4} \left[\mathcal{R}_2^{(+)}(\varepsilon_m, \varepsilon_n, -1) + \mathcal{R}_2^{(-)}(\varepsilon_m, \varepsilon_n, -1) \right] \\ = \frac{1}{4\sqrt{\pi}} \int_{1/\Lambda^2}^\infty \frac{du}{\sqrt{u}} \left(\frac{1}{u} \frac{e^{-u\varepsilon_n^2} - e^{-u\varepsilon_m^2}}{\varepsilon_m^2 - \varepsilon_n^2} - \frac{\varepsilon_n e^{-u\varepsilon_n^2} + \varepsilon_m e^{-u\varepsilon_m^2}}{\varepsilon_m + \varepsilon_n} \right). \quad (77)$$

It can be easily seen that the calculation of the moment of inertia is very similar to the case of the electric isovector form factor. Indeed, the Dirac sea contribution to the moment of inertia (21) can be written in the form:

$$\Theta^{sea} \delta_{ab} \int d\tau = \frac{N_c}{4} \frac{\partial^2}{\partial \epsilon_a \partial \epsilon_b} \text{Re} \text{Tr} \log(D_\epsilon^\dagger D_\epsilon)_{reg}, \quad (78)$$

where now

$$D_\epsilon = D(\bar{U}) - i\epsilon_c \tau^c. \quad (79)$$

Note that the first ϵ derivative in (78) can be interpreted as the derivative of the effective action with respect to the source to obtain the electric isovector form factor (at $q^2 = 0$) whereas the second ϵ derivative is analogous to the expansion in angular velocity. A detailed calculation including the valence quark contribution gives:

$$\Theta \delta_{ab} = \frac{N_c}{2} \left\{ \sum_{m \neq n} \langle m | \tau^a | n \rangle \langle n | \tau^b | m \rangle \mathcal{R}_\Theta^\Lambda(\varepsilon_m, \varepsilon_n) + \sum_{n \neq val} \frac{1}{\varepsilon_n - \varepsilon_{val}} \langle n | \tau^a | val \rangle \langle val | \tau^b | n \rangle \right\} \quad (80)$$

This regularized expression has been already derived in ref. [7] and numerically evaluated in refs. [8,12].

One can see from (76) and (80) that the isovector electric form factor has a proper normalization :

$$G_E^{T=1}(0) = 1 \quad (81)$$

as it should be.

Now we proceed to compute the magnetic form factors. From matrix element (67) and the definition of the magnetic Sachs form factor (71) we find that the first non-vanishing contributions come from rotational corrections:

$$G_M^{T=0}(q^2) = \frac{N_c \mathcal{M}_N}{6\Theta} \epsilon^{kaj} \frac{iq^j}{|q^2|} \int d^3x e^{i\vec{q}\vec{x}} \sum_{\substack{\varepsilon_n > \varepsilon_{val} \\ \varepsilon_m \leq \varepsilon_{val}}} \frac{\Phi_m^\dagger(\vec{x}) \gamma^0 \gamma^k \Phi_n(\vec{x}) \langle n | \tau^a | m \rangle}{\varepsilon_m - \varepsilon_n}. \quad (82)$$

The calculations of the magnetic isovector form factor are more involved and the final expression includes leading order terms as well as rotational corrections (next to leading order):

$$G_M^{T=1}(q^2) = \frac{N_c \mathcal{M}_N}{3} \epsilon^{kaj} \frac{iq^j}{|q^2|} \int d^3x e^{i\vec{q}\vec{x}} \left\{ [\Phi_{val}^\dagger(\vec{x}) \gamma^0 \gamma^k \tau^b \Phi_{val}(\vec{x})] - \sum_n \mathcal{R}_{M1}^\Lambda(\varepsilon_n) [\Phi_n^\dagger(\vec{x}) \gamma^0 \gamma^k \tau^b \Phi_n(\vec{x})] \right. \\ \left. - \frac{i}{2\Theta} \epsilon_{abc} \left[\sum_{n,m} \mathcal{R}_{M2}^\Lambda(\varepsilon_m, \varepsilon_n) [\Phi_m^\dagger(\vec{x}) \gamma^0 \gamma^k \tau^a \Phi_n(\vec{x})] \langle n | \tau^c | m \rangle - \sum_{\varepsilon_n \neq \varepsilon_{val}} \frac{\text{sign}(\varepsilon_n)}{\varepsilon_{val} - \varepsilon_n} [\Phi_n^\dagger(\vec{x}) \gamma^0 \gamma^k \tau^a \Phi_{val}(\vec{x})] \langle val | \tau^c | n \rangle \right] \right\}. \quad (83)$$

Here, two different regularization functions appear:

$$\mathcal{R}_{M1}^\Lambda(\varepsilon_n) = -\mathcal{R}_1(\varepsilon_n, 1) = \varepsilon_n \int_{-\infty}^{\infty} \frac{d\omega}{2\pi} \frac{e^{-(\omega^2 + \varepsilon_n^2)/\Lambda^2}}{\omega^2 + \varepsilon_n^2} = \frac{\varepsilon_n}{2\sqrt{\pi}} \int_{1/\Lambda^2}^{\infty} \frac{du}{\sqrt{u}} e^{-u\varepsilon_n^2}, \quad (84)$$

$$\mathcal{R}_{M2}^\Lambda(\varepsilon_m, \varepsilon_n) = \frac{1}{4} \left[-\mathcal{R}_2^{(+)}(\varepsilon_m, \varepsilon_n, 1) + \mathcal{R}_2^{(-)}(\varepsilon_m, \varepsilon_n, 1) \right] \\ = \frac{1}{4\pi} \int_0^1 \frac{d\beta}{\sqrt{\beta(1-\beta)}} \frac{(1-\beta)\varepsilon_m - \beta\varepsilon_n}{(1-\beta)\varepsilon_m^2 + \beta\varepsilon_n^2} e^{-[(1-\beta)\varepsilon_m^2 + \beta\varepsilon_n^2]/\Lambda^2}. \quad (85)$$

Eqs. (74), (76), (82) and (83) are our final expressions for the electromagnetic isoscalar and isovector form factors in the NJL model. According to (73) the proton and neutron form factors are expressed in terms of the isoscalar and isovector form factors as follows

$$G_{E(M)}^p = \frac{1}{2} [G_{E(M)}^{T=0} + G_{E(M)}^{T=1}], \quad (86)$$

$$G_{E(M)}^n = \frac{1}{2} [G_{E(M)}^{T=0} - G_{E(M)}^{T=1}]. \quad (87)$$

V. NUMERICAL RESULTS

In the numerical calculations we use the method of Ripka and Kahana [16] for solving the eigenvalue problem in finite quasi-discrete basis. We consider a spherical box of large radius D and the basis is made discrete by imposing a boundary condition at $r = D$. Also, it is made finite by restricting momenta of the basis states to be smaller than the numerical cut-off K_{max} . Both quantities have no physical meaning and the results should not depend on them. The typical values used are $D \sim 20/M$ and $K_{max} \sim 7M$.

In addition, all checks concerning the numerical stability of the solution with respect to varying box size and choice of the numerical cut-off have been done and the actual calculation is completely under control.

The parameters of the model are fixed in meson sector in the well known way [6] to have $f_\pi = 93$ MeV and $m_\pi = 139.6$ MeV. This leaves the constituent quark mass M as the only free parameter.

The proton and neutron electric and magnetic form factors are displayed in Figs.2-5. The theoretical curves resulting from the model are given for four different values of the constituent quark mass, namely 370, 400, 420 and 450 MeV. The

magnetic form factors are normalized to the experimental values of the corresponding magnetic moments at $q^2 = 0$. With one exception of the neutron electric form factor (Fig.3), all other form factors agree with the experimental data quite well. The best fit is for the constituent quark mass around 420 MeV.

As can be seen the only form factor which deviates from the experimental data is the neutron electric form factor and this requires some explanation. Obviously, this form factor is the most sensitive for numerical errors. According to the formula (87) the form factor has been calculated as a difference of the electric isoscalar and electric isovector form factors. Both form factors were of order of one and calculated by the code with high enough accuracy. However, the resulting neutron form factor has experimental values of order 0.04, *i.e.* about 4% of the value of its components. This means that even small theoretical uncertainties for one of the components can be enhanced by a factor 50. It means that the numerical accuracy together with the used large $1/N_c$ approximation behind the model are strongly magnified and could in principle result in a deviation from the experimental data for momentum transfers above 100 MeV. It should be also stressed that the experimental data (see ref. [18]), available for the neutron electric form factor, are strongly model dependent and a different $N - N$ potential used in the analysis of the data can lead to an enhancement of the experimental numbers by more than 50 %. There are also very recent experiment [19], which deviate from the previous data [18], indicating larger values closer to our numbers.

As the next step, we compute other electromagnetic observables: the mean squared radii, the magnetic moments and the nucleon- Δ splitting. In particular, the charge radii and the magnetic moments can be obtained from the form factors:

$$\langle r^2 \rangle_{T=0,1} = -\frac{6}{G_E^{T=0,1}} \frac{dG_E^{T=0,1}}{dq^2} \bigg|_{q^2=0}, \quad (88)$$

$$\mu^{T=0,1} = G_M^{T=0,1}(q^2) \bigg|_{q^2=0}. \quad (89)$$

For the quark masses 370, 420 and 450 MeV and pion mass $m_\pi = 140$ MeV the calculated values are presented in Table I. The values for the axial vector coupling constant g_A , taken from ref. [11], are also presented for completeness.

The results of Table I ($m_\pi = 139.6$ MeV) again indicate the value ~ 420 MeV for the constituent quark mass, in agreement with the conclusion drawn from the form factor curves. The same value has been suggested earlier [8,10], where a smaller number of observables has been considered. With the exception of the neutron electric squared radii, to which remarks similar to the case of the neutron electric form factor are valid, the contribution of the valence quarks is dominant. However, the contribution of the Dirac sea is non-negligible and it varies within the range 15 – 40%. As can be seen, the numerical results for the nucleon $N - \Delta$ mass splitting ($M_\Delta - M_N$), the mean squared proton, isoscalar and isovector electric radii and the axial coupling constant (g_A) as well as the q -dependence of the proton electric and magnetic, and neutron magnetic form factor differ from the experimental data by no more than about $\pm 5\%$. Finally, for the magnetic moments we have got results 20–25% below their experimental values. However, despite of this underestimation of both magnetic moments, we have found a very good result for the ratio μ_p/μ_n which is far better than in other models. The experimental ratio is almost exactly reproduced for the constituent quark mass 420 MeV.

In the present calculations, in contrast to the isoscalar magnetic moment the isovector one includes non-zero contributions in both leading (N_c^0) and next to leading order ($1/N_c$ rotational corrections). The enhancement due to these corrections improves considerably (see also ref. [11]) the agreement with the experiment and resolves to a great extent the problem of strong underestimation [12] of both the isovector magnetic moment and the axial vector coupling constant in leading order. It is also important to note that since the $1/N_c$ rotational corrections have the same spin-flavor structure like the leading term they do not violate the consistency condition of Dashen and Manohar [20] derived in the large- N_c of QCD. The latter means that other $1/N_c$ corrections (e.g. meson loops) should contribute to both the leading and next to leading order.

In Table II we give the theoretical values of the same quantities but with the physical pion mass set to zero. The chiral limit ($m_\pi \rightarrow 0$) mostly influences the isovector charge radius. In fact, as it should be expected [21,22], the isovector charge radius diverges in chiral limit and our calculations with zero pion mass confirms it. It can be seen in Fig.6, where the isovector charge radius is plotted *vs.* the box size D . The Dirac sea contribution to the radius grows linearly with D and diverges as $D \rightarrow \infty$. Because of this that quantity (and the relative quantities) is not included in Table II. The other observable strongly influenced by the chiral limit is the neutron electric form factor. For the $m_\pi \rightarrow 0$ the discrepancy from the experiment is by almost a factor two larger than in the case $m_\pi \neq 0$. The other observables differ in the chiral limit by about 30%. The comparison of the values in the two tables indicate that taking the physical pion mass gives us a best fit with a much better agreement with the experimental data. In addition, in chiral limit we observe much larger contribution from the sea effects, about 50% of the total value.

In section 3 we have found that the magnetic isovector form factor is the only one which includes non-zero contributions in both leading (N_c^0) and next to leading order ($1/N_c$) rotational corrections. However, the numerical calculations show that the $(1/N_c)$ rotational corrections do not affect the q^2 -dependence (slope) of the form factor but rather the value at the origin, $G_M^{T=1}(0) = \mu^{T=1}$ which is the isovector magnetic moment. It is not surprising since (as can be seen from eq. (83) in both leading and next to leading order terms the shape of the wave functions Φ_n determines the q^2 -dependence of the form factor whereas the value at $q^2 = 0$ depends on the particular matrix elements included. In leading order the isovector magnetic moment is strongly underestimated [12]. As has been shown in ref. [11] the enhancement for this quantity due to the $1/N_c$ corrections is of order $(N_c + 2)/N_c$ and it improves considerably the agreement with experiment. However, as can be seen from Table I the magnetic moments are still below the experimental value by 25 %.

The isoscalar and isovector electric mean squared radii are shown in Figs.7,8 as functions of the constituent quark mass. The same plot for the proton and neutron electric charge radii is given in Fig.9. In these plots the valence and sea contributions are explicitly given (dashed and dash-dotted lines, respectively). As could be expected, for the isoscalar electric charge radius the valence part is dominant (about 85%), due to the fact that there is no $1/N_c$ rotational contributions. This is not true for the isovector electric charge radius, where the sea part contributes to about 45% of the total value (Fig.7). Also, this effect can be seen at the proton and neutron charge radii (Fig.9) which are linear combinations of the isoscalar and isovector ones. For proton the sea contribution is about 30% whereas for the neutron charge radius the negative sea part is dominating and the valence contribution is negligible.

In addition, in Fig.10 we plot the proton and neutron charge distribution for the constituent quark mass $M = 420$ MeV. For the proton we have a positive definite charge distribution completely dominated by the valence contribution whereas in the case of the neutron the Dirac sea is dominant. In accordance with the well accepted phenomenological picture one realizes a positive core coming from the valence quarks and a long negative tail due to the polarization of the Dirac sea. Using the gradient expansion the latter can be expressed in terms of the dynamical pion field – pion cloud.

For completeness, in Fig.11 we present also the magnetic moment density distribution for proton and neutron for the constituent quark mass $M = 420$ MeV. The sea contribution becomes non-negligible for distances greater than 0.5 fm. Due to the relatively large tail contribution to the magnetic moments the sea contribution to these quantities is about 30%.

VI. SUMMARY AND CONCLUSIONS

Our numerical results support the view that the chiral quark soliton model of the SU(2) Nambu–Jona-Lasinio type offers relatively simple but quite successful description of some low-energy QCD phenomena and, in particular, of the nucleon electromagnetic properties. In calculations, using $f_\pi = 93$ MeV, $m_\pi = 139.6$ MeV and a constituent quark mass of $M = 420$ MeV, and no other parameters, we have obtained an overall good description for the electromagnetic form factors, the mean squared radii, the magnetic moments, and the nucleon– Δ splitting. The isoscalar and isovector electric radii are reproduced within 15%. The magnetic moments are underestimated by about 25%. However, their ratio μ_p/μ_n is almost perfectly reproduced. To this end, the account of the $1/N_c$ rotational corrections is decisive. The q -dependence of $G_E^p(q^2)$, $G_M^p(q^2)$ and $G_M^n(q^2)$ is very well reproduced up to momentum transfer of 1 GeV. The only exception is the neutron form factor $G_E^n(q^2)$ which is by a factor of two too large for $q^2 > 100$ MeV 2 . One should note, however, that $G_E^n(q^2)$ is more than an order of magnitude smaller than $G_E^p(q^2)$ and as such it is extremely sensitive to both the model approximations and the numerical methods used. Here, it turns out that the agreement is noticeably worse if the chiral limit ($m_\pi \rightarrow 0$) is used. This can be easily understood since the pion mass determines the asymptotic behavior of the pion field. Altogether we conclude that the chiral quark soliton model based on a bosonized SU(2) NJL type lagrangean is quite appropriate for the evaluation of nucleonic electromagnetic properties.

Acknowledgement:

The project has been partially supported by the BMFT, DFG and COSY (Jülich). Also, we are greatly indebted for financial support to the Bulgarian Science Foundation Φ-32 (CVC) and to the Polish Committee for Scientific Research, Projects KBN nr 2 P302 157 04 and 2 0091 91 01 (AZG).

[1] Y.Nambu and G.Jona-Lasinio, *Phys.Rev.* **122** (1961) 354
[2] T.Eguchi, H.Sugawara, *Phys.Rev.* **D10** (1974) 4257; T.Eguchi, *Phys.Rev.* **D14** (1976) 2755

- [3] D.Diakonov, V.Petrov, *Phys.Lett.* **147B** (1984) 351; *Nucl.Phys.* **B272** (1986) 457; Quark Cluster Dynamics, eds. K.Goeke, P.Kroll,H.-R.Petry, Lecture Notes in Physics, Springer-Verlag, v.417, 1992, p.288
- [4] D.I.Diakonov, V.Yu.Petrov and P.V.Pobylitsa, 21st LNPI Winter School on Elem.Part. Physics, Leningrad 1986; *Nucl.Phys.* **B306**(1988)809;
- [5] H.Reinhardt and R.Wünsch, *Phys.Lett.* **215B**(1988)577; ibid. **B230** (1989) 93
- [6] T.Meissner, F.Grümmer and K.Goeke, *Phys.Lett.* **227B** (1989) 296; *Ann.Phys.* **202** (1990) 297; T.Meissner and K.Goeke, *Nucl.Phys.* **A254** (1991) 719
- [7] H.Reinhardt, *Nucl.Phys.* **503B**(1989)825
- [8] K.Goeke, A.Z.Górski, F.Grümmer, Th.Meissner, H.Reinhardt, R.Wünsch, *Phys.Lett.* **B256** (1991) 321
- [9] T.Meissner and K.Goeke, *Z.Phys.***A339**(1991)513
- [10] A.Z.Górski, K.Goeke, F.Grümmer, *Phys.Lett.* **B278** (1992) 24
- [11] Chr.V.Christov, A.Blotz, K.Goeke, V.Yu.Petrov, P.V.Pobylitsa, M.Wakamatsu, T.Watabe, *Phys.Lett.* **B325**(1994)467
- [12] M.Wakamatsu, H.Yoshiki, *Nucl.Phys.* **A524** (1991) 561
- [13] M.-C.Chu, J.M.Grandy, S.Huang and J.W.Negele, *Phys.Rev.* **D49** (1994) 6039
- [14] R.Ball, *Phys.Rep.* **182** (1989) 1
- [15] M.Schaden, H.Reinhardt, P.Amundsen, M.Lavelle, *Nucl.Phys.* **B339** (1990) 595
- [16] S.Kahana and G.Ripka, *Nucl.Phys.***A429** (1984) 462
- [17] G.Höhler at al., *Nucl.Phys.***B414** (1976) 505
- [18] S.Platchkov at al., *Nucl.Phys.***A510** (1990) 740
- [19] T.Eden at al., *Phys.Rev.***C50** (1994) R1749
- [20] R.Dashen and A.V.Manohar, *Phys.Lett.***315B** (1993) 425, 438
- [21] M.A.Bet and A.Zepeda, *Phis.Rev.* **D6** (1972) 2912
- [22] G.S.Adkins, C.R.Nappi and E.Witten, *Nucl.Phys.* **B228** (1983) 552

FIG. 1. Diagrams corresponding to the expansion in Ω of the current matrix element: a) the valence contribution and b) the Dirac sea contribution.

FIG. 2. The proton electric form factor for the momentum transfers below 1 GeV. Experimental data from ref. [17].

FIG. 3. The neutron electric form factor for the momentum transfers below 1 GeV. experimental data from refs. [18,19].

FIG. 4. The proton magnetic form factor normalized to the experimental value of the proton magnetic moment at $q^2 = 0$ for the momentum transfers below 1 GeV. The normalization factor can be extracted from Table 1. Experimental data from ref. [17].

FIG. 5. The neutron magnetic form factor normalized to the experimental value of the neutron magnetic moment at $q^2 = 0$ for the momentum transfers below 1 GeV. The normalization factor can be extracted from Table 1. Experimental data from ref. [17].

FIG. 6. The isovector charge radius as a function of the box size D for $m_\pi = 0$ and $m_\pi = 139.6$ MeV.

FIG. 7. The isoscalar electric charge radius as a function of the constituent quark mass M . The valence and sea parts are marked by the dashed and dashed-dotted lines.

FIG. 8. The isovector electric charge radius as a function of the constituent quark mass M . The valence and sea parts are marked by the dashed and dashed-dotted lines.

FIG. 9. The electric charge radii of proton and neutron as functions of the constituent quark mass M . The valence and sea parts are marked by the dashed lines.

FIG. 10. The charge density distribution of the proton (lower) and neutron (upper) for the constituent quark mass $M = 420$ MeV.

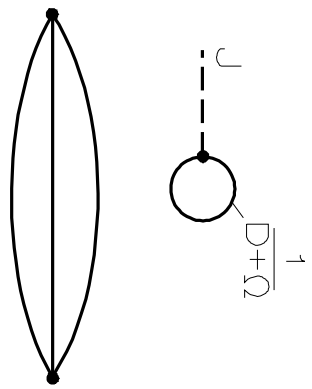
FIG. 11. The magnetic moment density of proton and neutron for the constituent quark mass $M = 420$ MeV.

TABLE I. Nucleon observables calculated with the physical pion mass.

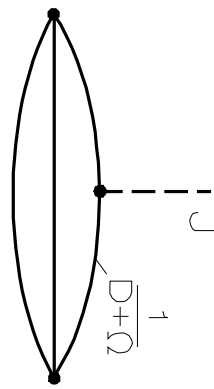
Quantity	Constituent Quark Mass						Exper.	
	370 MeV		420 MeV		450 MeV			
	total	sea	total	sea	total	sea		
$\langle r^2 \rangle_{T=0}$ [fm 2]	0.63	0.05	0.52	0.07	0.48	0.09	0.62	
$\langle r^2 \rangle_{T=1}$ [fm 2]	1.07	0.33	0.89	0.41	0.84	0.45	0.86	
$\langle r^2 \rangle_p$ [fm 2]	0.85	0.19	0.70	0.24	0.66	0.27	0.74	
$\langle r^2 \rangle_n$ [fm 2]	-0.22	-0.14	-0.18	-0.17	-0.18	-0.18	-0.12	
$\mu_{T=0}$ [n.m.]	0.68	0.09	0.62	0.03	0.59	0.05	0.88	
$\mu_{T=1}$ [n.m.]	3.56	0.77	3.44	0.97	3.16	0.80	4.71	
μ_p [n.m.]	2.12	0.43	2.03	0.50	1.86	0.43	2.79	
μ_n [n.m.]	-1.44	-0.34	-1.41	-0.47	-1.29	-0.38	-1.91	
$ \mu_p/\mu_n $	1.47	—	1.44	—	1.44	—	1.46	
$\langle r^2 \rangle_p^\mu$ [fm 2]	1.08	0.32	0.66	0.28	0.56	0.25	0.74	
$\langle r^2 \rangle_n^\mu$ [fm 2]	1.17	0.51	0.65	-0.31	-0.52	-0.24	-0.77	
$M_\Delta - M_N$ [MeV]	213	—	280	—	314	—	294	
g_A	1.26	0.08	1.21	0.11	1.13	0.06	1.26	

TABLE II. Nucleon observables calculated with the zero pion mass.

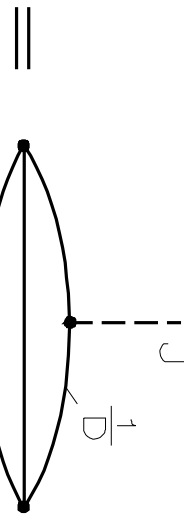
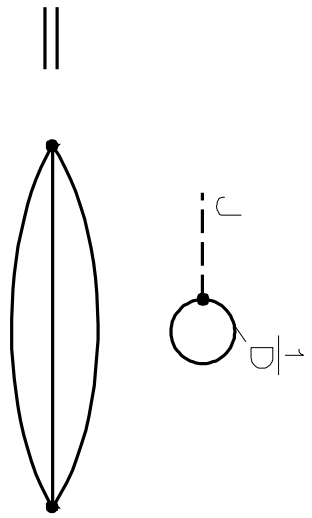
Quantity	Constituent Quark Mass						Exper.	
	370 MeV		420 MeV		450 MeV			
	total	sea	total	sea	total	sea		
$\langle r^2 \rangle_{T=0}$ [fm 2]	0.88	0.20	0.66	0.26	0.61	0.23	0.62	
$\mu_{T=0}$ [n.m.]	0.66	0.07	0.59	0.09	0.57	0.09	0.88	
$\mu_{T=1}$ [n.m.]	4.61	1.59	4.38	1.89	3.91	1.48	4.71	
μ_p [n.m.]	2.63	0.83	2.49	0.99	2.24	0.79	2.79	
μ_n [n.m.]	-1.97	-0.76	-1.89	-0.90	-1.67	-0.70	-1.91	
$ \mu_p/\mu_n $	1.34	—	1.34	—	1.34	—	1.46	
$M_\Delta - M_N$ [MeV]	221	—	261	—	301	—	294	



\square



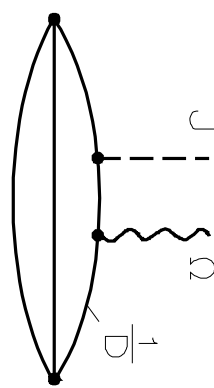
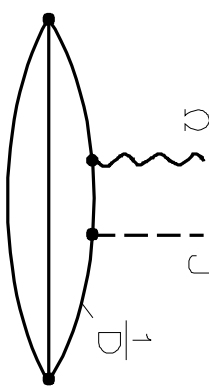
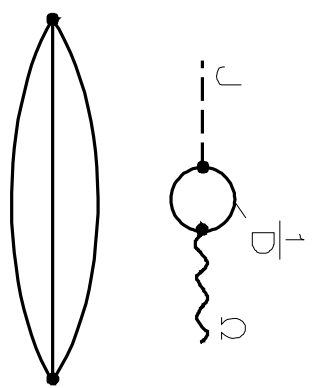
∂

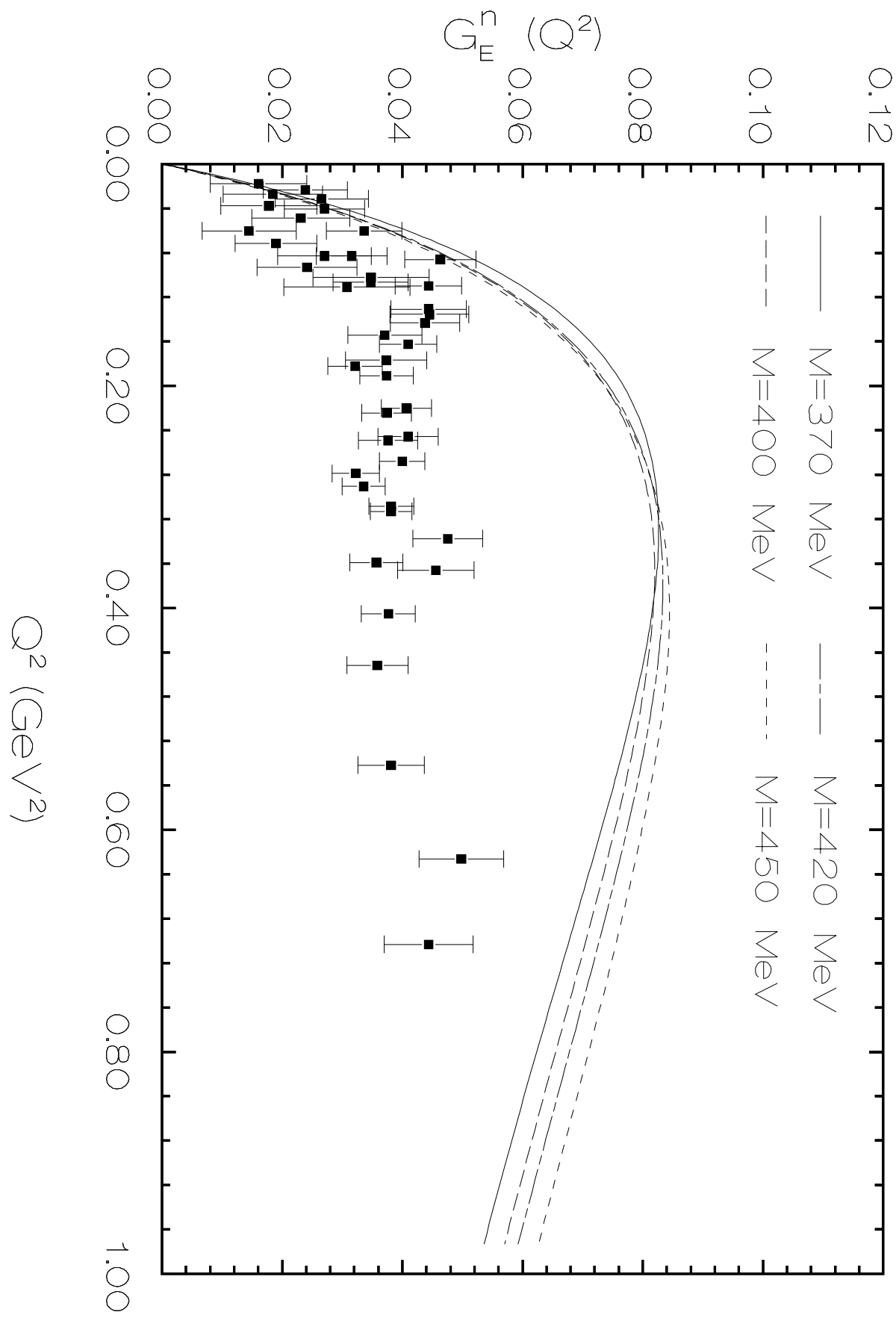


$+$

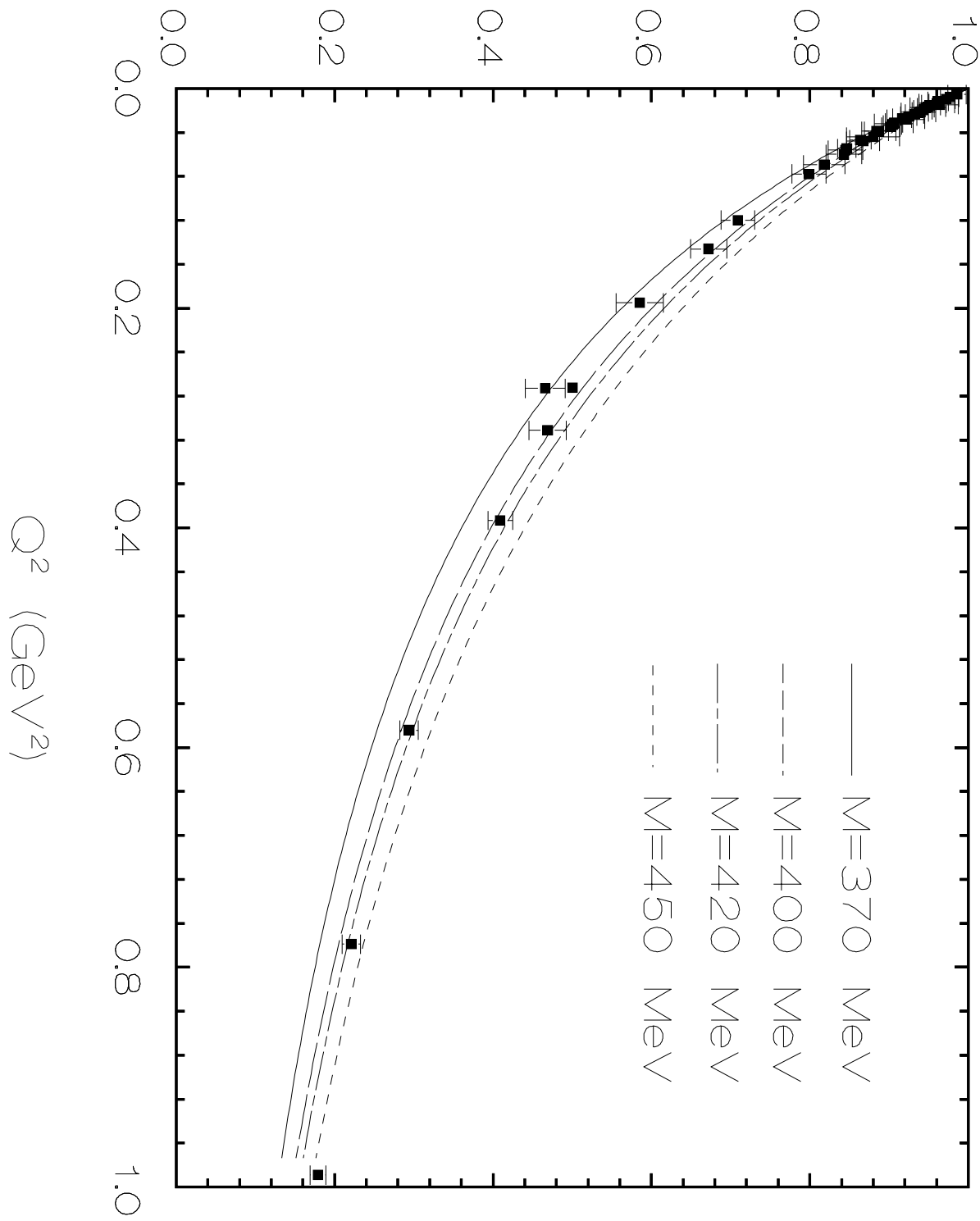
$+$

$+$

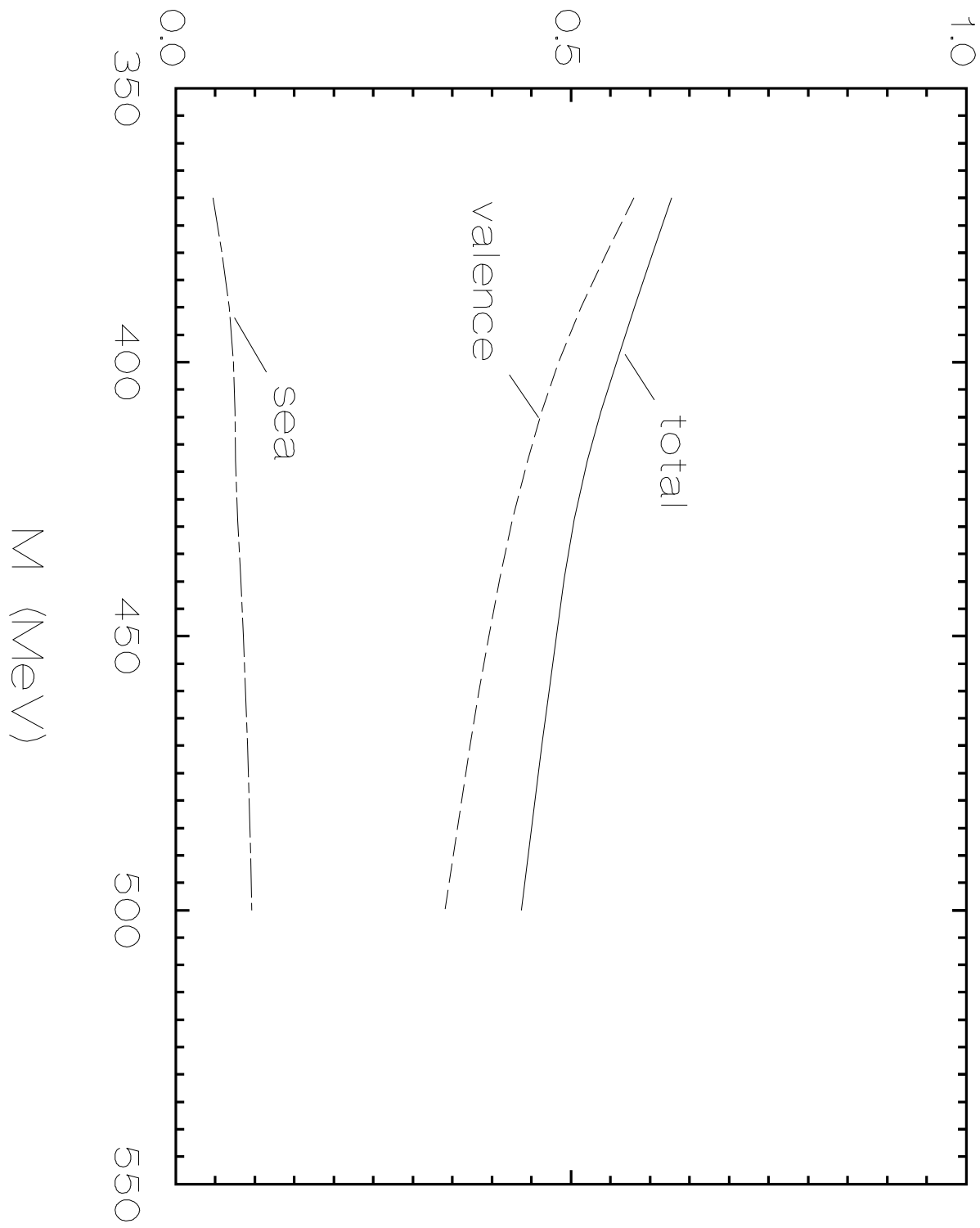




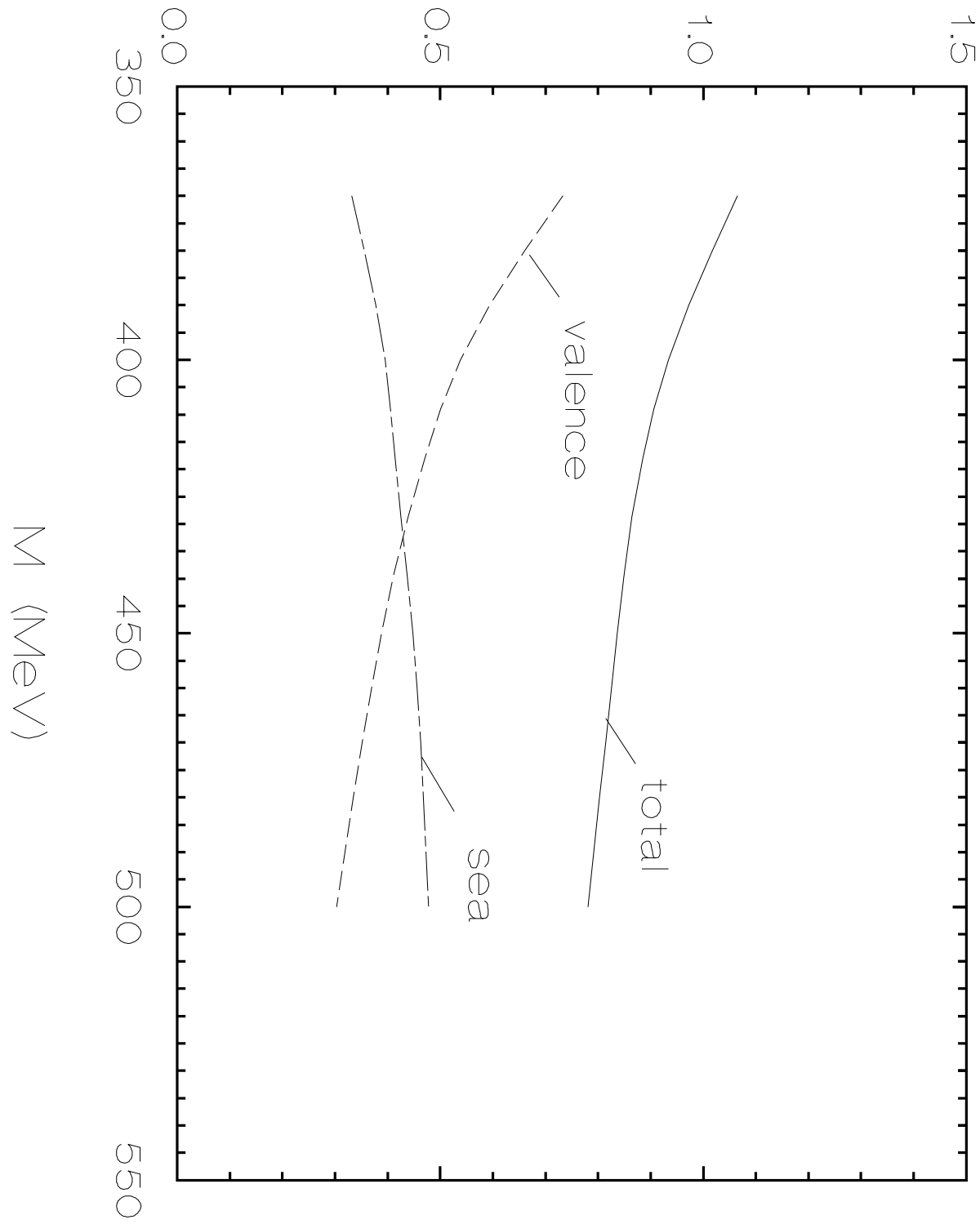
$$G_E^p(Q^2)$$

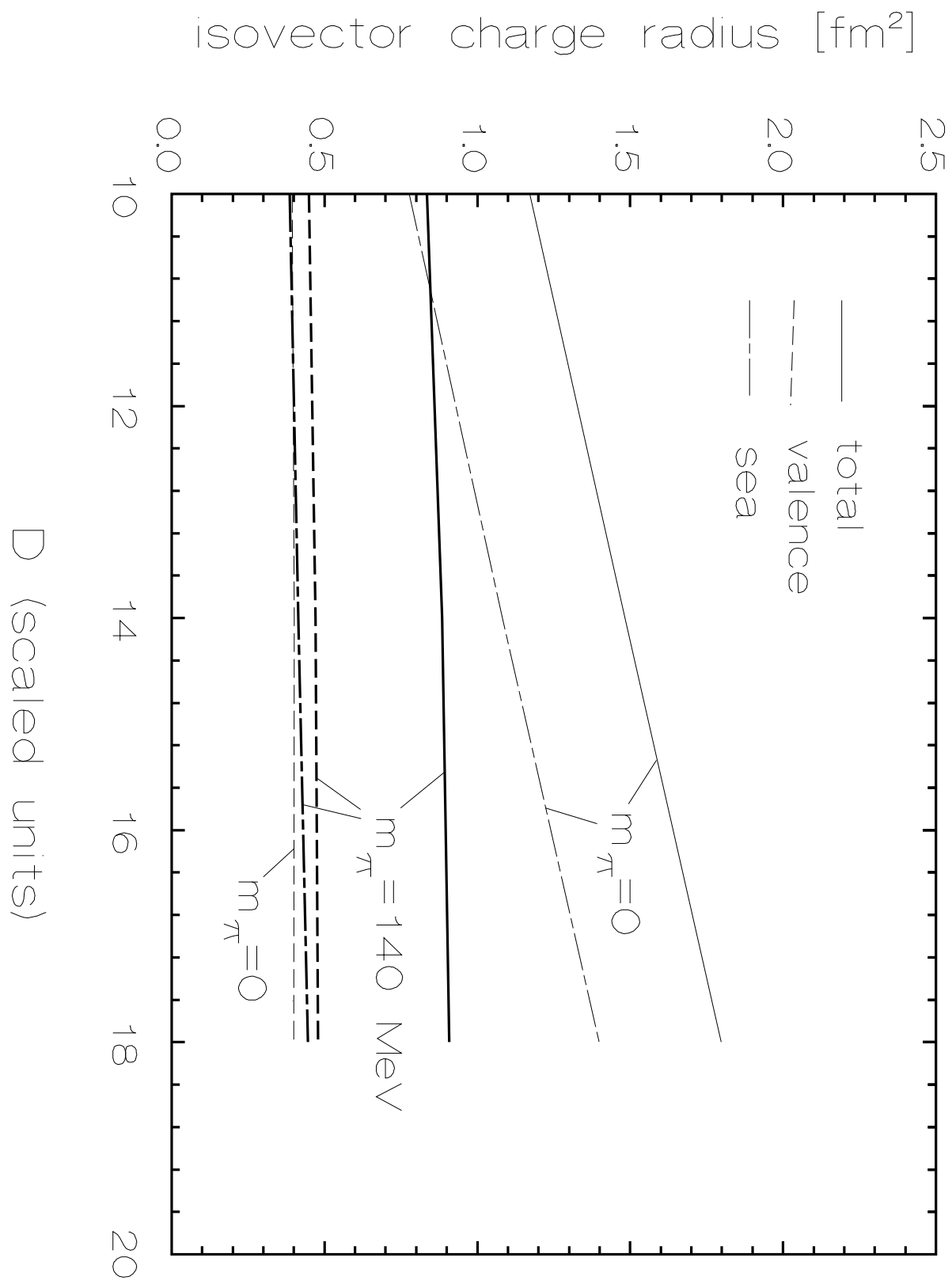


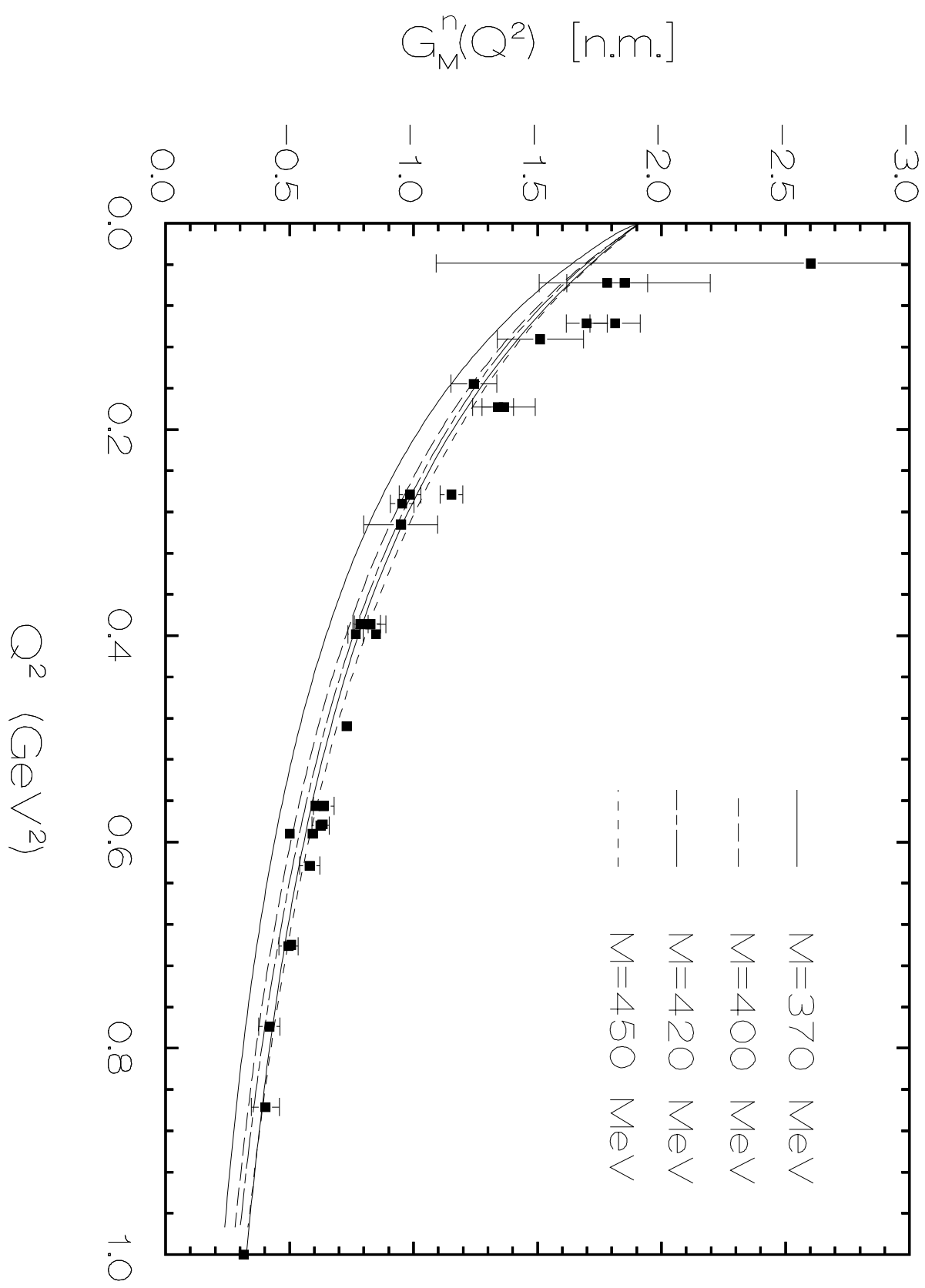
isoscalar charge radius [fm^2]

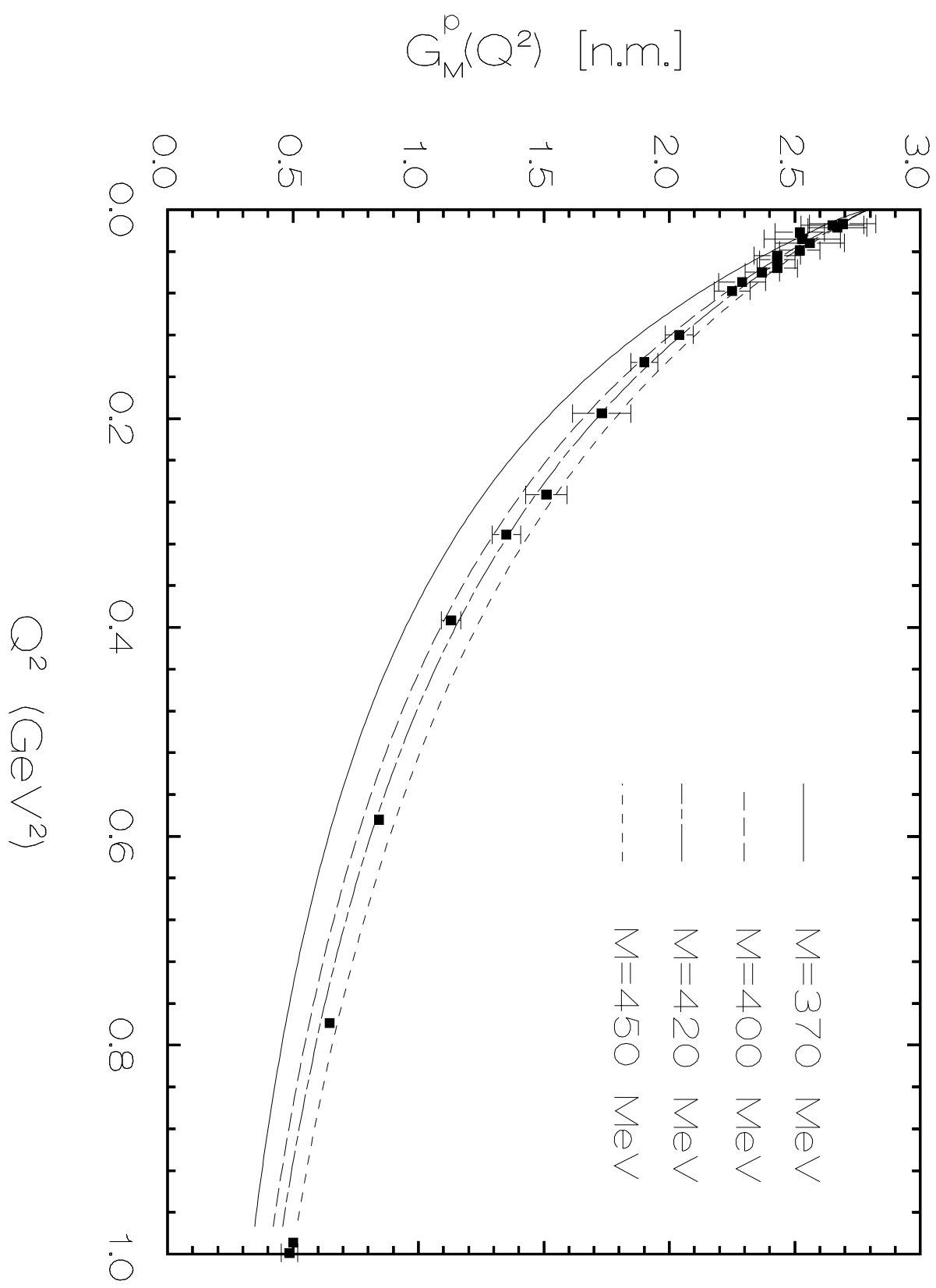


isovector charge radius [fm²]









isovector magnetic moment in NJL
model in linear rotational order

